Surface Enhanced Raman Spectroscopy on Single Mode Nanophotonic-Plasmonic Waveguides

F. Peyskens[1], **A. Dhakal**[1], **P. Van Dorpe**[2], **N. Le Thomas**[1], **R. Baets**[1]

[1] *Photonics Research Group, INTEC-department, Ghent University-imec; Center for Nano-and BioPhotonics, Ghent University, Sint-Pietersnieuwstraat 41, 9000 Ghent, Belgium*

[2] *imec, Kapeldreef 75, 3001 Heverlee, Belgium; Department of Physics, KULeuven, Celestijnenlaan 200D, 3001 Leuven, Belgium*

frederic.peyskens@ugent.be

Abstract: We analyze the generation of Surface Enhanced Raman Spectroscopy signals from integrated bowtie antennas, excited and collected by a single mode silicon nitride waveguide, and discuss strategies to enhance the Signal-to-Noise Ratio.

OCIS codes: (130.3120) Integrated optics devices, (250.5403) Plasmonics, (300.6450) Spectroscopy, Raman

1. Introduction

Surface Enhanced Raman Spectroscopy (SERS) is a well-established technique to enhance Raman spectra by introducing a resonant metallic nanostructure near the analyte under study [1, 2]. SERS signals are however mainly generated and collected by bulky and expensive microscopy systems. The development of photonic integrated circuits functionalized with dedicated nanoplasmonic structures would present a major step towards the realization of dense SERS probes which allow multiplexed detection of extremely weak Raman signals. To this end, we analyze the generation of Surface Enhanced Raman Spectroscopy signals from integrated bowtie antennas, excited and collected by a single mode silicon nitride waveguide (Fig. 1(a)) [3], and discuss strategies to enhance the Signal-to-Noise Ratio.

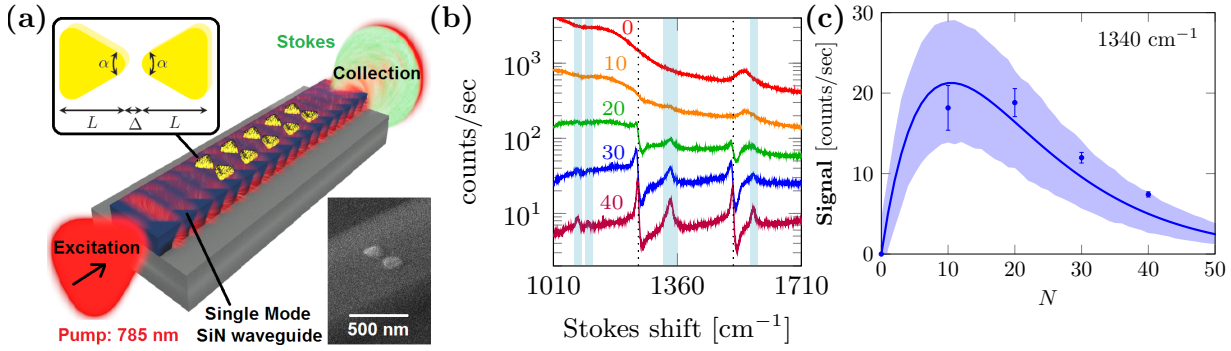

Fig. 1: **(a)** Silicon nitride (SiN) waveguide functionalized with an array of N bowtie antennas. The bottom inset shows a SEM image of an integrated bowtie antenna. **(b)** SERS spectra of waveguides functionalized with a varying number of N ($N = 0, 10, 20, 30, 40$) bowtie antennas with $\alpha \approx 60°$, $L \approx 106 \pm 8$ nm and $\Delta \approx 48 \pm 13$ nm. **(c)** Signal strength of the 1340 cm^{-1} peak as a function of N (points). The solid curve represents a fit of the experimental data to a theoretical model, developed in [3], which describes the on-chip SERS effects. The shaded area incorporates the theoretical impact of disorder in the system [3].

The antennas were coated with 4-nitrothiophenol (NTP), which selectively binds to gold. As such, any Raman signal results from the surface enhancement effect near the gold and does not contain other contributions. A TE-polarized $\lambda_P = 785$ nm pump laser is used to excite the antennas. NTP Raman spectra collected from waveguides functionalized with a varying number of antennas N are shown in Fig. 1(b). The cyan shaded areas mark the spectral positions where an NTP Stokes peak is expected, while the peaks denoted by the black dashed lines result from interference effects generated by the Au array [3]. While the non-functionalized ($N = 0$) reference waveguide does not generate any NTP SERS signal, it does generate a relatively large Raman signal background originating from the SiN waveguide core (with length ≈ 1 cm). The shot noise associated to this background limits the detection of the weakest NTP Raman

peaks as shown in Fig. 1(b) where the smallest 1110 cm^{-1} feature only appears for the $N = 40$ waveguide. The Signal-to-Noise Ratio (*SNR*) of this feature improves due to the background attenuation induced by the increasing number of antennas. However, the absolute signal strength decreases when N becomes too large (see Fig. 1(c)). This originates from the interplay between signal generation and pump and Stokes attenuation induced by the antennas [3]. As a result, reducing the signal background by increasing the number of antennas will typically reduce the absolute signal strength as well.

2. Backward scattering and noise reduction

In order to minimize the background without jeopardizing the absolute Raman signal strength, we designed a Y-splitter where the antenna array is patterned on the straight arm ($\approx 120\ \mu m$) of the splitter (Fig. 2(a) bottom). The total length of all arms equals $L_Y \approx 1$ cm.

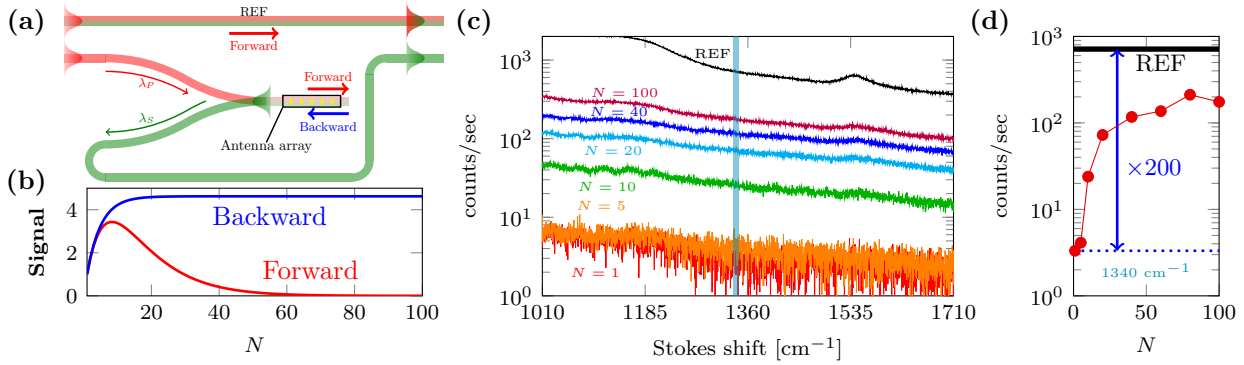

Fig. 2: **(a)** (top) Straight reference waveguide REF with copropagating pump and Stokes; (bottom) Y-splitter design separating pump and Stokes beam. **(b)** Theoretical comparison between forward and backward on-chip SERS scattering. **(c)** Backward scattered Raman spectra of a Y-splitter functionalized with varying N. For comparison, the forward scattered Raman spectrum of a straight reference waveguide (REF) is also added. The cyan shaded area marks the 1340 cm^{-1} region. **(d)** Zoom on the background of the 1340 cm^{-1} region.

The rationale for using such a design is twofold. At first, the SERS signal is collected in backward scattering, i.e. pump and Stokes beam are counterpropagating, because backward scattering is always larger than forward scattering (see Fig. 2(b)). Hence, the absolute signal strength is improved. This can be understood from the fact that the signal from the first antenna, which is the strongest, is fully available at the output, as opposed to the forward scattering case from Fig. 1(c). The signal from subsequent antennas will then experience an ever increasing attenuation by the previous antennas, such that the backscattering signal eventually saturates for a sufficiently large number of antennas. Secondly, the unwanted silicon nitride background has to be separated from the SERS light in order to mitigate the shot noise associated with the background. This can be achieved by injecting the pump in the upper arm and collecting the backscattered SERS light in the bottom arm. Part of the background light that is generated in the upper arm can however reflect, either on the antenna array or the back facet of the straight arm, and propagate back into the bottom arm. Moreover the pump beam is partially reflected into the bottom arm, where it generates background light as well. Initial experiments already prove that the background can be effectively reduced, as shown in Fig. 2(c) where the backward scattered Raman spectra of a Y-splitter functionalized with varying N are plotted. For comparison, we also added the forward scattered Raman spectrum of a straight reference waveguide REF (Fig. 2(a) top) whose total length equals L_Y. A zoom on the 1340 cm^{-1} region is shown in Fig. 2(d). Compared to the reference waveguide, a 200-fold background reduction is found for the $N = 1$ case. In contrast to the previous case, the background decreases when N decreases. This trend is ascribed to reflections caused by the antenna array.

Currently we are improving this design in order to optimize the *SNR*, which ultimately should enable the detection of extremely weak Raman signals from a single antenna. This would allow quantitative and multiplexed detection of several biological and chemical substances, such as viruses or DNA, on a fully integrated platform.

References

1. J. N. Anker, et al. "Biosensing with plasmonic nanosensors," Nat. Mater. **7**, 442–453 (2008).
2. N. J. Halas, et al. "Plasmons in strongly coupled metallic nanostructures," Chem. Rev. **111**, 3913–3961 (2011).
3. F. Peyskens, et al. "Surface Enhanced Raman Spectroscopy Using a Single Mode Nanophotonic-Plasmonic Platform," ACS Photonics **3(1)**, 102–108 (2016).